Semi-Lagrangian Particle Methods for Hyperbolic Equations

Georges-Henri Cottet

Abstract Particle methods with remeshing of particles at each time-step can be seen as forward semi-lagrangian conservative methods for advection-dominated problems, and must be analyzed as such. In this article we investigate the links between these methods and finite-difference methods and present convergence results as well as techniques to control their oscillations. We emphasize the role of the size of the time-step and show that large time-steps, only limited by the flow strain, can lead to significant gains in both computational cost and accuracy. Our analysis are illustrated by numerical simulations in level set methods and in fluid mechanics for compressible and incompressible flows.

1 Particle methods for conservation laws

Particle methods have long been considered as natural tools for the discretization of conservation laws, written in general form as

$$\frac{\partial \mathbf{U}}{\partial t} + \text{div}\,(\mathbf{a} : \mathbf{U}) + \mathbf{A}\mathbf{U} = \mathbf{F} \tag{1}$$

In the above equation $\mathbf{U}$ is a vector in $\mathbf{R}^m$, $\mathbf{a} = (a_j)$ is a vector field in $\mathbf{R}^n$ and

$$\text{div}\,(\mathbf{a} : \mathbf{U}) = \left(\sum_{j=1}^{n} \partial (a_j u_i) / \partial x_j \right)_{i \in [1,m]}.$$

The term $\mathbf{F}$ represents both external forces and terms that are not related to advection, typically diffusion terms or pressure gradients. This PDE translates the follow-

Georges-Henri Cottet
University Grenoble Alpes and Institut Universitaire de France e-mail: georges-henri.cottet@univ-grenoble-alpes.fr

ing conservation property

$$\frac{d}{dt}\left[\int_{\Omega(t)} \mathbf{U}\, d\mathbf{x}\right] + \int_{\Omega(t)} \mathbf{A}\mathbf{U}\, d\mathbf{x} = \int_{\Omega(t)} \mathbf{F}\, d\mathbf{x}$$

where $\Omega(t)$ is a domain of $\mathbf{R}^n$ moving with velocity $\mathbf{a}$. System (1) must of course be supplemented by boundary conditions (at least inflow boundary condition in case $\mathbf{F} = 0$). However we will here focus on unbounded problems, or problems with periodic boundary conditions.

Particle methods consist of concentrating the mass of $\mathbf{U}$ on points (particles), which means that the following approximation is considered :

$$\mathbf{U}_h(\mathbf{x},t) = \sum_p \alpha_p(t)\delta(\mathbf{x} - \mathbf{x}_p(t)). \tag{2}$$

Particle trajectories are along the velocity field

$$\frac{d\mathbf{x}_p}{dt} = \mathbf{a}(\mathbf{x}_p,t)$$

and particle strengths change to account for zero order terms and right hand side $\mathbf{F}$. When smooth quantities must be recovered/plotted one can rely on mollified particles (or blobs)

$$\mathbf{U}_h^\varepsilon(\mathbf{x},t) = \sum_p \alpha_p(t)\zeta_\varepsilon(\mathbf{x} - \mathbf{x}_p(t)) \tag{3}$$

where $\zeta_\varepsilon(\mathbf{x}) = \varepsilon^{-n}\zeta(\mathbf{x}/\varepsilon)$ with ζ a smooth function satisfying $\int \zeta(\mathbf{x})\, d\mathbf{x} = 1$.

The strengths of the particles represent local masses. It may be convenient to write these masses in terms of local values of $\mathbf{u}$ and local volumes :

$$\alpha_p(t) = \mathbf{U}(\mathbf{x}_p(t),t)v_p(t)$$

with

$$\frac{dv_p}{dt} = \mathrm{div}\mathbf{a}(\mathbf{x}_p,t)v_p.$$

In case of an incompressible flow ($\mathrm{div}\,\mathbf{a} = 0$), strengths, local values and volumes of the particles are conserved along the flow.

The velocity field, as well as the matrix $\mathbf{A}$ and the right hand side $\mathbf{F}$ can either be given (linear problems) or function of the solution $\mathbf{U}$ (nonlinear problems). In the latter case the coupling of the advected quantities with the flow field (in particular) requires to consider the mollified particle distribution, which, as we will see below, has important consequences on the convergence properties of the method.

1.1 Classical examples

In the linear case, passive scalars advected by a flow, like concentration or density in incompressible flows or level set functions to capture an interface, are natural examples. Scalars which feedback to the flow, like temperature or density in compressible flows, or interface capturing level set functions in presence of surface tension, are non-linear examples where particle methods can been used.

More elaborate examples include the Vlasov-Maxwell system, the Navier-Stokes equations in vorticity form and the equations of gas dynamics.

In the Vlasov-Maxwell system the advected quantity is the density probability f associated to each specie of ions or electrons, moving under the action of the electric and magnetic fields. The phase-space variables are the positions and velocities (in other words $n = 6$ in the general case). The conservation law for f can be written as (1) with $\mathbf{a}(\mathbf{x},\mathbf{v}) = (\mathbf{v}, \mathbf{E}(\mathbf{x},t) + \mathbf{v} \times \mathbf{B}(\mathbf{x},t))$, $\mathbf{A} = \mathbf{F} = 0$ (assuming an elementary electric charge equal to 1). The electric and magnetic fields are computed from the momentum of f with respect to $\mathbf{v}$ (charge density and electric current) through the Maxwell equations. We refer to [14, 4] for descriptions and numerical analysis of particle methods in this context.

Inviscid incompressible flows can be described by the vorticity form of the incompressible Euler equations [5]. In this case, $n = m = 3$, $\mathbf{U} = \boldsymbol{\omega} = \nabla \times \mathbf{u}$, $\mathbf{a} = \mathbf{u}$ and $\mathbf{A} = [\partial u_i / \partial x_j]$. For the Navier-Stokes equations, viscosity and diffusion come in the right hand side $\mathbf{F}$. Note that in two dimensions, it is convenient to represent the vorticity as a vector along the axis perpendicular to the flow plane. In this case the so-called stretching term $\mathbf{AU}$ vanishes and the mass of the particles coincide with the local circulation of the flow. In 3D the stretching term is responsible for reorientation and amplification of the local vorticity, and ultimately of the onset of 3D turbulence.

Finally gas dynamics equations can be recast in terms of density, momentum and energy : $\mathbf{U} = (\rho, \rho\mathbf{u}, \rho E)$, which in the most general case gives $m = 5$ and $n = 3$. The term $\mathbf{F}$ is made of pressure gradients terms to complete the momentum and energy equations. Its discretization by means of particles led to Smooth Particle Hydrodynamics (SPH) methods [22].

1.2 Sketch of numerical analysis and overlapping condition

To give an idea of the numerical analysis of these methods, let us assume for a sake of simplicity a linear equation where $\mathbf{A} = \mathbf{F} = 0$. One way to understand the convergence properties of particle methods [6] is to realize that particle approximation given by (2) are *exact* weak solutions to the advection equation (1). One can further show that, for smooth enough velocity fields, the advection equation is stable in distribution spaces of the form $W^{-m,p}(\mathbf{R}^n)$. As a result one can write

$$\|(\mathbf{U} - \mathbf{U}_h)(\cdot,t)\|_{W^{-m,p}} \leq \exp(CT)\, \|(\mathbf{U} - \mathbf{U}_h)(\cdot,0)\|_{W^{-m,p}}$$

where C depends on the derivatives of $\mathbf{a}$. If at $t = 0$ particles are initialized on a regular grid of grid-size h and if the initial condition is of class C^∞ with compact support (or periodic) the right hand side above can be bounded through classical quadrature rules by $O(h^m)$ for arbitrary m, which gives

$$\|(\mathbf{U} - \mathbf{U}_h)(\cdot, t)\|_{W^{-m,p}} = 0(h^m).$$

Now, to obtain error bounds in L^p norms for the mollified particles (3), one needs to add regularization errors and to "pay the price" for the mollification. This easily leads to the following estimate

$$\|(\mathbf{U} - \mathbf{U}_h^\varepsilon)(\cdot, t)\|_{W^{-m,p}} \leq \exp(CT)(\varepsilon^r + h^m/\varepsilon^m)$$

where r is such that $\int \mathbf{x}^\gamma \zeta(\mathbf{x})\, d\mathbf{x} = 0$ for $1 \leq |\gamma| \leq r-1$. The above estimate exhibits two scales in the convergence process : ε, the mollifying range, which eventually dictates the overall order of the method, and h the particle spacing. It also shows that convergence requires $h \ll \varepsilon$, or in other words that many particles lie in the mollifying range. In case the right hand side $\mathbf{F}$ involves pressure gradients or diffusion term, one can easily predict that this overlapping condition will be even more demanding. A more precise analysis also shows that the flow strain (derivatives of the velocity) is responsible for the exponential term in the error estimate which indicates that the overlapping requirement gets more difficult to fulfill in presence of strong shear in the flow.

2 From grid-free to semi-lagrangian particles

The overlapping condition just outlined has long been recognized as a major difficulty to perform accurate simulations, in particular for non-linear problems. Figure 1 illustrates typical numerical artifacts appearing in he simulation of a smooth axisymmetric (and thus steady) vortex for the incompressible 2D Euler equations when the blob size ε remains constant and of the order of the initial particle spacing. The situation is even more problematic when the nonlinearity does not involve any smoothing effect, unlike in the case of incompressible flows in vorticity formulation just mentioned or for the Vlasov-Poisson equations. In that case the flow strain prohibits any convergence proof. This includes the simple 1D Burger's equations. As a matter of fact, convergence analysis in the SPH literature (e.g. [1]) always assume that particles are carried by a smooth flow field and focus on the particle treatment of pressure gradient terms.

An important effort has been made starting in the 80's to overcome this difficulty for flow simulations. In particular a class of methods aims at adapting the particle weights or mollifying range to the local flow strain (see [5] and the references therein). Triangulated particle methods for vortex methods [27] or renormalization methods for gas dynamics [23] fall in this category. More recently [26], methods have been designed in particular to improve the treatment of diffusion with grid-

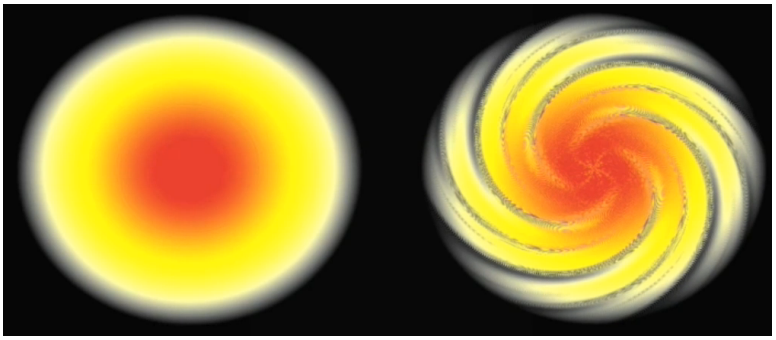

Fig. 1 Numerical artifact due to a lack of overalapping in the simulation of a steady smooth axisymmetric vortex in the 2D incompressible Euler equation (curtesy of P. Koumoutsakos). Left picture : exact solution; right picture : numerical solution with $\varepsilon \simeq h$.

free particles. However these methods have been mostly validated for 2D flows and it is not clear that they offer viable tools (in terms of accuracy ad cost) for complex 3D flows.

An alternative approach consists of remeshing particles from time to time in order to maintain the initial overlapping. This strategy can be traced back to inviscid equations and the first vortex sheet calculations [17] or vortex filament calculations [21]. In these cases particles where lying on curves and the overlapping could be maintained by simply inserting fresh particles when successive particles were too far apart. The weights of the fresh particles could easily be computed by interpolation along filaments (in 3D) or sheets (in 2D). For more general vortex topology and/or to handle the Navier-Stokes equations, a more systematic approach, together with appropriate treatment of boundary conditions, was introduced and implemented for flow past 2D cylinders at high Reynolds numbers in [15] and for the study of the axisymmetrization of elliptical vortices in [16], where it allowed to obtain reference results. These calculations were soon followed by 3D simulations [24, 25, 9].

Until recently particle remeshing was considered as an *ad hoc* fix, to maintain the regularity of the particle distribution at the price of some truncation error every *few* time steps. In practice, the number of time-steps between two successive remeshing steps never increases as the particle spacing tends to zero, which means that the remeshing error cannot be considered as an additional truncation error but must be analyzed as part of the particle scheme. On the other hand the time scale which governs the particle distortions is of order $\|\nabla \mathbf{u}\|_{L^\infty}^{-1}$, similar to the time-scale which is used for the time-discretization of the particle motion. As a result, these time-scales are routinely taken equal which means that remeshing is performed at each time-step. It is important to point out that this particular implementation offers several additional advantages. It allows particle methods to be combined with grid-based methods when appropriate, either in the same computational domain (for example to rely on FFTs to compute velocity or electric/magnetic fields) or in domain-

decomposition approaches [24]. It also enables Adaptive Mesh Refinement [2] or wavelet-based multilevel [3] approaches.

For advection equations with uniform grids, the resulting method becomes a *forward*, *conservative* semi-lagrangian method and must be analyzed as such.

3 Semi-lagrangian particle methods for linear hyperbolic equations

In he following we denote by Δx the grid size and Δt the time-step. Let us consider the following one-dimensional advection equation in conservation form

$$\frac{\partial u}{\partial t} + \text{div}\ (au) = 0, x \in \mathbf{R}, t > 0, \tag{4}$$

where a is a given smooth velocity field. Assuming that particles are initialized and remeshed on a uniform grid with grid-size Δx, we obtain

$$u_i^{n+1} = \sum_j u_j^n \Gamma\left(\frac{x_j^{n+1} - x_i}{\Delta x}\right), i \in \mathbf{Z}^d, n \geq 0, \tag{5}$$

where Γ is the interpolation function used to remesh particles. In the above equation

$$x_i^{n+1} = x_i + \tilde{a}_i^n \Delta t, \tag{6}$$

where $\tilde{a}_i^n$ is the velocity field used to push particle and depends on the chosen time-stepping scheme. As we will see later, the construction of accurate interpolation kernels is done by requiring the conservation of successive moments of the particle distribution. This means that Γ satisfies

$$\sum_{k \in \mathbf{Z}} (x-k)^\alpha \Gamma(x-k) = \begin{cases} 1 & \text{if } \alpha = 0 \\ 0 & \text{if } 1 \leq \alpha \leq p \end{cases}, x \in \mathbf{R}, \tag{7}$$

for some value of $p \geq 1$. The simplest example of interpolation kernel is the piecewise linear function which conserves mass $\sum_i u_i^n$ and first momentum $\sum x_i u_i^n$ ($p = 1$). In the case of constant velocity this choice corresponds, for a CFL number less than 1, to the classical first order upwind scheme. However it is readily seen that this choice can lead to inconsistency if the local CFL number crosses an integer value, in particular when the velocity changes sign, whatever time-step is chosen. For instance for $a(x) = x$, a particle initialized and remeshed at $x = 0$ will keep its strength unchanged although the exact solution at this point is given by $u_0(x)\exp(-t)$.

The number of integers inside the support of Γ must increase with p. The choice $p = 2$ leads to a piecewise quadratic function, with support on three grid points, which yields the following weights (according to Figure 2)

$$\alpha_j = -\lambda(1-\lambda)/2\ ,\ \beta_j = 1-\lambda^2\ ,\ \gamma_j = \lambda(1+\lambda)/2, \tag{8}$$

where λ is the algebraic distance, normalized by Δx, between the particle, after advection, and the nearest grid point. For a constant velocity and a CFL number below 1/2, this formula corresponds to the Lax-Wendroff finite-difference scheme [8]. However, for CFL numbers larger than $1/2$, this kernel can lead to inconsistencies which can be corrected by first order terms [20].

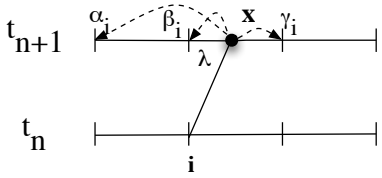

Fig. 2 Sketch of advection-remeshing with a 3-points formula.

The consistency issues just mentioned are actually related to the lack of regularity of the kernels : the piecewise linear kernel is not differentiable, and the piecewise quadratic kernel is not even continuous. Indeed, requiring more regularity, together with moment properties and the interpolation property, which means that remeshing does not change the weights if particles do not move, allows to prove a general consistency theorem [10]. Under the following assumptions

Γ is even and piecewise polynomial in intervals of the form $[i, i+1]$,
Γ is of class C^r, for $r \geq 1$
Γ satisfies the moment properties (7) for $p \geq 1$,
Γ satisfies the interpolation property $\Gamma(i-j) = \delta_{i,j}, i, j \in \mathbf{Z}$

and provided the time step Δt satisfies the following condition (sometimes referred to as a Lagrangian CFL condition)

$$\Delta t < |a'|_{L^\infty}^{-1}, \tag{9}$$

one can prove that, for an Euler time-stepping scheme for the motion of particles, the consistency error of the semi-lagrangian method is bounded by $O(\Delta t + \Delta x^\beta)$ where $\beta = \min(p, r)$. Moreover, at least for kernels of order up to 4, under appropriate decay properties for the kernel Γ one can prove the stability of the method under the sole assumption (9). Higher order in time can be recovered by using classical Runge-Kutta methods to push particles. The kernel conditions listed above can be used to construct in a systematic fashion high order kernels, denoted $\Lambda_{p,r}$ (see in [10] examples for β up to 6).

The above discussion concerns 1D equations but carries on to several dimensions using directional splitting for advection equations. In practice it means that particles are transported then remeshed in successive directions, with the possibility of using

high order splitting methods. As a mater of fact, dimensional splitting allows to use high order (with large support) kernels at an affordable cost.

Figure 3 presents a comparaison between computed and exact solutions in the classical level set case of a disk undergoing filamentation in the velocity field resulting from a smooth off-center vortex. The particle method uses the 4th order kernel $\Lambda_{6,4}$, 256^2 points and a CFL number equal to 30. For this experiment, a second order directional splitting and a 4th order Runge Kutta method were used and the observed order of accuracy was 5.9 (we refer to [10] for more examples and refinement studies). Figure 4 shows a comparison of the efficiency of kernels $\Lambda_{2,1}$ and $\Lambda_{8,4}$ for a similar 3D experiment, with 256^3 points and a CFL number equal to 30.

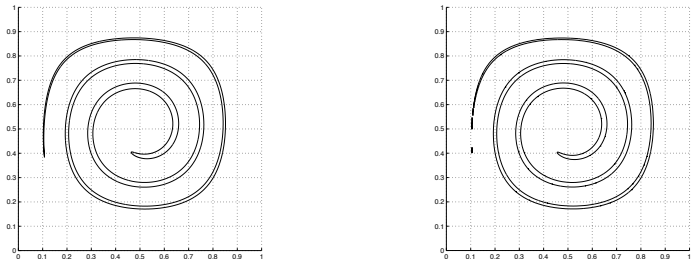

Fig. 3 Advection of a level set in a 2D off-center vorticity field [10]. Comparison of the exact solution (left) and 4th-order particle solution using $N = 256^2$ particles and a CFL number equal to 30.

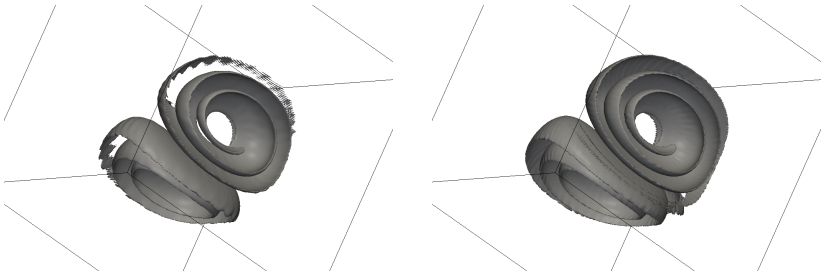

Fig. 4 Advection of a level set in a 3D off-center vorticity field [10]. Comparison of the results obtained by a 1st order and 4th order kernels, using $N = 256^3$ particles with a CFL number equal to 30.

A striking example where the combination of high-order accuracy and large time-steps can lead to very efficient implementations of semi-lagrangian particle methods is the study of scalar turbulence. In the passive advection of a scalar in a turbulent flow, when the diffusivity of the scalar is smaller than the viscosity of the flow, the spectrum of the scalar exhibits a k^{-1} decay range, beyond the classical $k^{-5/3}$ range of the flow. This implies that, for Direct Numerical Simulations, it is necessary to use a finer resolution for the scalar than for the flow. The ratio of the flow viscosity to the scalar diffusivity is called the Schmidt number (Sc) and the ratio between the corresponding grid discretizations has to be of the order of $\sqrt{Sc}$. Using semi-lagrangian particles allows to increase the scalar resolution while keeping time steps defined by the flow strain and not by the fine particle discretization. In [18] systematic simulations coupling semi-lagrangian particles for the scalar and spectral methods for the flow, allowed to exhibit the k^{-1} scalar spectrum decay for a large range of Schmidt numbers and to confirm the Kraichnan prediction for the dissipative scales of the scalar (see Figure 5). In the case of a Schmidt number equal to 128, resolutions of up to 3000^3 were made possible because the time-step could be larger than what would be necessary in a spectral method by a factor close to 100. Figure 6 shows scalar and vorticity contours in a periodic turbulent plane jet [13],

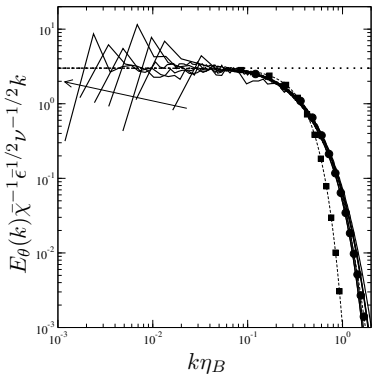

Fig. 5 Scalar spectra compensated by k for different Schmidt numbers [18] (arrow indicates increasing values of Sc). The squares (resp. dots) indicates the Batchelor (resp. Kraichnan) prediction of the dissipative scales.

for a Reynolds number equal to 10^3 and a Schmidt number equal to 64. This simulation used semi-lagrangian particles both for the vorticity to solve the Navier-Stokes equations, and for the scalar, respectively at grid resolutions of 128^3 and 1024^3. The flow and scalar particles were computed on different hardware, to account for the different parallel scalability of te different parts of the algorithm : 8 CPUs for the flow and 8 GPUs for the scalar for a computational cost of about 1.5 second per iteration.

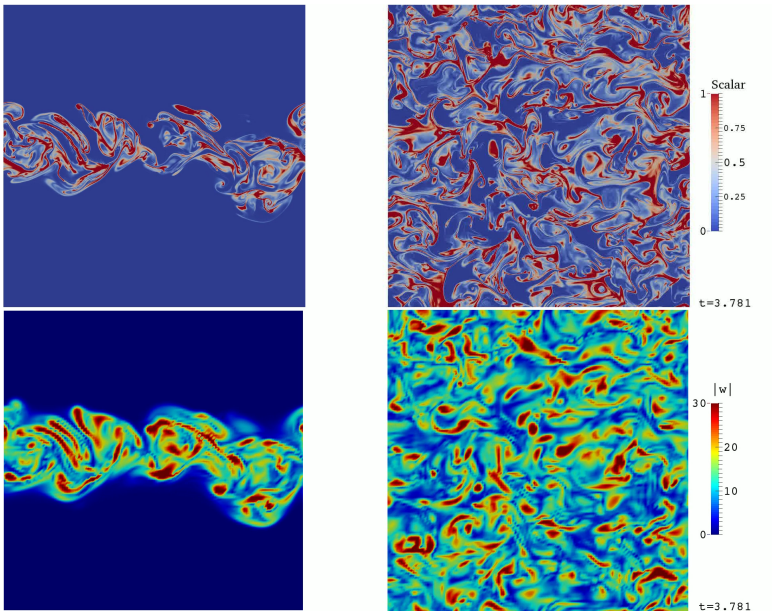

Fig. 6 Periodic plane jet for $Re = 10^3$ and $Sc = 64$ [13]. Side (left) and top (right) views showing the different scales in the vorticity (bottom) and the scalar (top). Simulation with 128^3 particles for the flow and 1024^3 particles for the scalar.

4 Semi-Lagrangian particles for nonlinear conservation laws

Let us first consider scalar equations of the form

$$u_t + (g(u)u)_x = 0. \tag{10}$$

The situation is different from the linear case. If one considers the piecewise linear remeshing kernel together with an explicit first order time-discretization, it is easy to see that, for a CFL number smaller than 1, it translates into the following 3 points scheme :

$$u_j^{n+1} = u_j^n - \lambda \left[u_{j+1} g_{j+1}^- + u_j g_j^+ - u_j g_j^- - u_{j-1} g_{j-1}^+ \right], \tag{11}$$

where $\lambda = \Delta t / \Delta x$ and the superscript $+$ and $-$ denote the positive and negative parts. This scheme has a numerical flux given by

$$F(u,v) = ug(u)^+ + vg(v)^-$$

and is therefore consistent with the original equation. Let us now consider the three-points second order formula (8) associated to the piecewise quadratic kernel corresponding to the Lax-Wendroff scheme in the constant coefficient case. To obtain a second order scheme both in time and space, one can consider a Runge Kutta scheme

where the particle velocities are predicted by advancing the equation for half a time-step. That can be done using the following approximation for the particle velocity at time $(t_n + t_{n+1})/2)$ [7]

$$u_j^{n+1/2} = u_j^n \left(1 - \Delta t\, g(u)_x(x_j)/2\right). \tag{12}$$

In practice $g(u)_x(x_j)$ in the above formula is evaluated by a centered finite difference $(g(u_{j+1}^n) - g(u_{j-1}^n))/(2\Delta x)$. The finite-difference formula corresponding to this method for a CFL number below $1/2$ can be then derived along the same lines as in the linear case and is given by

$$\begin{aligned} u_j^{n+1} = u_j^n &- \frac{\Delta t}{2\Delta x}(\tilde{g}_{j+1}^n u_{j+1}^n - \tilde{g}_{j-1}^n u_{j-1}^n) \\ &+ \frac{\Delta t^2}{2\Delta x^2}\left((\tilde{g}_{j+1}^n)^2 u_{j+1}^n - 2(\tilde{g}_j^n)^2 u_j^n + (\tilde{g}_{j-1}^n)^2 u_{j-1}^n\right) \end{aligned} \tag{13}$$

where we have set $\tilde{g}_j^n = g(u_j^{n+1/2})$. It can be checked [8, 28] that this is a second order scheme.

For systems of conservation laws, the above ideas extend to flux splitting methods, where advective fluxes are dealt with by semi-lagrangian particles, whereas pressure gradient terms are handled by grid-based finite-volume methods. These methods bear some similarities with the Advection Upstream Splitting Method [19], with the difference that in our case the advection does not involve the pressure flux in the energy equation. It also can be seen as a variation of the Lagrange-projection methods [12], with the difference that in our case the advection step is performed in the conservation form. Note that, in the case of systems, the up-winding implicitly resulting from particle motions is based on material velocities and not on wave speeds. Figure 7 shows a comparison of a semi-lagrangian particle method using the $\Lambda_{2,1}$ kernel with a Mac-Cormack scheme using a third-order limiter derived in [11] for the calculation of the interaction of a shock wave with a boundary layer of a Reynolds number of 200, with the same grid resolution $\Delta x = 10^{-3}$.

5 Non-oscillatory semi-lagrangian particles

Like all high order methods, semi-lagrangian particle methods can produce spurious oscillations near sharp variations of the solution. To prevent this, limiters can be derived in a similar way to finite-differences schemes. The general idea is to start from the equivalent finite-difference scheme when the CFL number is below a certain value, to derive limiters for these schemes and to go back to remeshing formulas by interpreting the modified finite-difference coefficients.

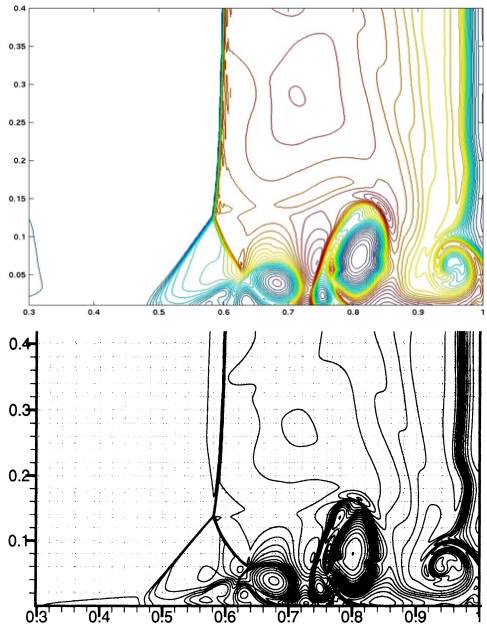

Fig. 7 Density levels in a shock / boundary layer interaction. Comparison of the results of a semi-lagrangian particle method (top) and of the third order Mc Cormack finite-difference scheme [11] (bottom). In both calculations $\Delta x = 10^{-3}$.

5.1 The linear case

In that section we give the derivation of [20] for non-oscillatory remeshing schemes obtained by limiting 2nd order centered formulas with first order centered formulas. More specifically, since we have seen above that the piecewise linear remeshing is not consistent for non constant velocities, we choose a 3 points first order centered formula. For $|\lambda = a\Delta t/\Delta x| \leq 1/2$, with the the notations of Figure 8 the weights corresponding to this remeshing kernel are given by :

$$\alpha_j = 3/4 - \lambda^2 \ , \ \beta_j = 1/2(1/2-\lambda)^2 \ , \ \gamma_j = 1/2(1/2+\lambda)^2.$$

This is equivalent to a first order scheme written in incremental form as

$$u_j^{n+1} = u_j^n + C^{(1)}_{j+1/2}\Delta v_{j+1/2} - D^{(1)}_{j-1/2}\Delta v_{j-1/2}$$

where $\Delta v_{j+1/2} = v_{j+1} - v_j$ and

$$C^{(1)}_{j+1/2} = 1/2(\lambda - 1/2)^2 \ , \ D^{(1)}_{j-1/2} = 1/2(\lambda + 1/2)^2$$

Similarly, the second order remeshing scheme (8), which corresponds to the Lax-Wendroff scheme when $|\lambda| \leq 1/2$, can be recast in a similar incremental form with coefficients $C^{(2)}_{j+1/2} = C^{(1)}_{j+1/2} - 1/8$ and $D^{(2)}_{j-1/2} = D^{(1)}_{j-1/2} - 1/8$. It is therefore natural to look for TDV scheme of the form

$$u_j^{n+1} = u_j^n + C^{(1)}_{j+1/2}\Delta v_{j+1/2} - D^{(1)}_{j-1/2}\Delta v_{j-1/2} - \frac{1}{8}\phi_{j+1/2}\Delta v_{j+1/2} + \frac{1}{8}\phi_{j-1/2}\Delta v_{j-1/2} \tag{14}$$

where, classically, ϕ is a function of the slopes with values in $[0,1]$. To derive appropriate TVD conditions for ϕ let us first assume that $\lambda \geq 0$. We then define $\phi_{j+1/2} = \phi(r_{j+1/2})$ where $r_{j+1/2} = \Delta v_{j+1/2}/\Delta v_{j-1/2}$ and rewrite (14) as

$$u_j^{n+1} = u_j^n + \frac{1}{2}(\lambda - 1/2)^2\Delta v_{j+1/2} - \Delta v_{j-1/2}[\frac{1}{2}(\lambda + 1/2)^2 + \frac{1}{8}\phi_{j-1/2} - \frac{1}{8}\frac{\phi_{j+1/2}}{r_{j+1/2}}].$$

Using Harten's theorem it is readily seen that we obtain a TVD scheme provided ϕ satisfies $|\phi(s) - \phi(r)/r| \leq 1$ which allows to use the classical limiters. This scheme can be interpreted back into a remeshing formula with weights (according to Figure 2) given by

$$\begin{aligned}
\alpha_j &= \frac{1}{2}(\lambda - \frac{1}{2})^2 - \frac{1}{8}\phi_{j-1/2}, \\
\beta_j &= \frac{3}{4} - \lambda^2 + \frac{1}{8}(\phi_{j-1/2} + \phi_{j+1/2}), \\
\gamma_j &= \frac{1}{2}(\lambda + \frac{1}{2})^2 - \frac{1}{8}\phi_{j+1/2}.
\end{aligned}$$

If $\lambda \leq 0$ we rewrite (14) as

$$u_j^{n+1} = u_j^n + \frac{1}{2}(\lambda + 1/2)^2\Delta v_{j-1/2} - \Delta v_{j+1/2}[\frac{1}{2}(\lambda - 1/2)^2 - \frac{1}{8}\phi_{j+1/2} - \frac{1}{8}\frac{\phi_{j-1/2}}{\tilde{r}_{j-1/2}}]$$

where $\tilde{r}_{j-1/2} = \Delta v_{j+1/2}/\Delta v_{j-1/2}$. Remeshing weights are then given by a formula similar to the ones above.

The point is now that the resulting scheme can be used even for a CFL number larger than one (in this case one has to use the corrected Λ_2 formula derived in [7]). The method then of course does not reduce anymore to a finite-difference scheme. To illustrate the method we consider the case of a double top-hat function advected in a flow with a positive velocity with sinusoidal modulation [20]. This flow, although very smooth, results in compression and dilatation, associated to an increase or decrease of local values, which are delicate to capture. Figure 8 shows a comparison, with the same grid size $\Delta x = 0.510^{-2}$, of the non-oscillatory particle scheme at a CFL number equal to 12, with a 5th-order WENO scheme for a CFL number equal to 2. Strikingly the particle scheme performs better, although it is at most second order and locally only first order. The reason is that, because it uses large time-steps, it "sticks" more to the exact condition.

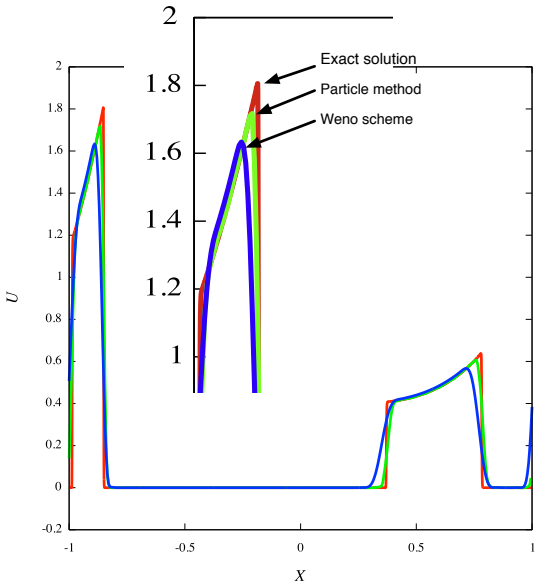

Fig. 8 Comparison of a semi-lagrangian particle method (green curve) and a 5th-order weno scheme (blue curve), using the same grid-size, with the exact solution (red curve), for the advection of a double top-hat function in a sinusoidal velocity field [20]. The CFL number for the particle method is 12.

5.2 The non-linear case

The above discussion extends to the non-linear case [7, 28]. [28] in particular contains a detailed derivation of the TVD formulas associated to a large class of first and second order remeshing kernels, for scalar conservation laws and for the Euler equations. It also gives a proof, for these TVD particle schemes, of convergence towards entropy solutions in the case of scalar equations. Note that, to our knowledge, this is the only convergence proof of particle methods for non-linear scalar conservation laws.

Unlike in the case of linear equations, these schemes are restricted to CFL conditions similar to the finite-difference methods. Indeed, due to the shocks, the Lagrangian CFL condition, where the time-step is constrained by flow derivatives, reduce in this case to a classical CFL condition since the flow derivatives can reach values of the order of $\max|u|/\Delta x$. In Figure 9 we show an illustration of a TVD semi-lagrangian particle scheme for a classical shock tube. In this example the particle scheme uses the second order formula (8), corresponding to the second order scheme (13), limited by the upwind first order piecewise linear formula (corresponding to (11)) and the pressure gradient terms are computed using the first order method in the Euler-Lagrange method in [12]. This illustration shows that, in con-

trast with the linear case, the method does not avoid the numerical dissipation of first order schemes, in particular in the contact discontinuity. Based on the preceding remarks concerning the linear case, one may expect that using local time steps, with CFL numbers larger than 1 away from shocks, could improve this part of the solution. This possibility has yet to be tested.

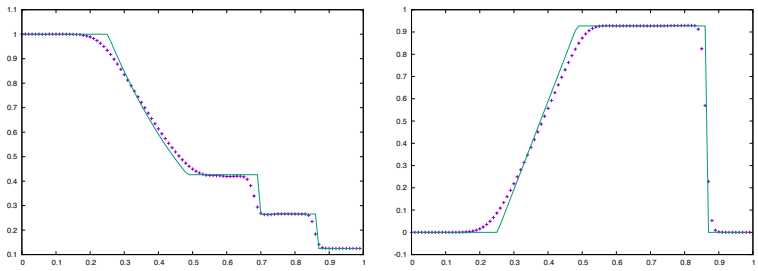

Fig. 9 Semi-lagrangian particle solution (red dots) for a shock-tube problem, compared to the exact solution (green curve), for $\Delta x = 10^{-2}$. Left picture : density; right picture : velocity.

6 Conclusion

Particle methods with particle remeshing at each time-step can be analyzed as semi-lagrangian conservative methods. High order methods can be easily implemented and the analogy with finite-differences for small time-steps enables the derivation of non-oscillatory schemes. For linear problems, the possibility to use large times-steps, only constrained by the flow strain, can lead to significant savings. For non-linear problems, the method can be seen as a particular case of advective flux-splitting. Using local time-steps or decoupling the scales of the conservative variables and of the velocity field are two possible directions to enhance the performance of the methods.

References

1. B. Ben Moussa and J.-P. Vila, *Convergence of SPH method for scalar nonlinear conservation laws*, SIAM Journal on Numerical Analysis, 37, 863–887 (2000).
2. M. Bergdorf, G.-H. Cottet and P. Koumoutsakos, *Multilevel Adaptive Particle Methods for Convection-Diffusion Equations*, SIAM Multiscale Modeling and Simulation, 4, 328–357, 2005.
3. M. Bergdorf and P. Koumoutsakos, *A Lagrangian Particle-Wavelet Method*, SIAM Multiscale Modeling and Simulation, 5(3), 980–995 (2006).
4. G-H Cottet, P-A Raviart, *Particle methods for the one-dimensional Vlasov-Poisson equations*, SIAM Journal on Numerical Analysis, 21, 52–76 (1984).

5. G.-H. Cottet and P. Koumoutsakos, Vortex methods, Cambridge University Press, 2000.
6. G.-H. Cottet, *A new approach for the analysis of vortex methods in 2 and 3 dimensions*, Ann. Inst. Henri Poincaré, 5, 227–285 (1988).
7. G.-H. Cottet and A. Magni, *TVD remeshing schemes for particle methods*, C. R. Acad. Sci. Paris, Ser. I, 347 (2009).
8. G.-H. Cottet and L. Weynans, *Particle methods revisited: a class of high-order finite-difference schemes*, C. R. Acad. Sci. Paris, Ser. I 343, 51–56 (2006).
9. G.-H. Cottet, B. Michaux, S.Ossia and G. Vanderlinden, *A comparison of spectral and vortex methods in three-dimensional incompressible flows*, J. Comp. Phys, 175, 2002.
10. G.-H. Cottet, J.-M. Etancelin, F. Perignon and C. Picard, *High order Semi-Lagrangian particles for transport equations: numerical analysis and implementation issues*, ESAIM: Mathematical Modelling and Numerical Analysis, 48, 1029–1060 (2014).
11. V. Daru and C. Tenaud, *Evaluation of TVD high resolution schemes for unsteady viscous shocked flows*, Computers & Fluids, 30, 89–113 (2001).
12. B. Despres and F. Lagoutiere, *Contact discontinuity capturing schemes for linear advection and compressible gas dynamics*, J. Sci. Comput. 16, 479–524 (2002).
13. J.-M. Etancelin, G.-H. Cottet, F. Perignon and C. Picard, *Multi-CPU and multi-GPU hybrid computations of multi-scale scalar transport*, 26th International Conference on Parallel Computational Fluid Dynamics, 2014, Trondheim.
14. R.W. Hockney and J.W. Eastwood , Computer Simulation Using Particles, McGraw-Hill Inc., 1981.
15. P. Koumoutsakos and A. Leonard, *High Resolution simulations of the flow around an impulsively started cylinder using vortex methods*, J. Fluid Mech., 296, 1–38 (1995).
16. P. Koumoutsakos, *Inviscid Axisymmetrization of an Elliptical Vortex*, J. Comp. Physics,138, 821–857 (1997).
17. R. Krasny, *Desingularization of periodic vortex sheet roll-up*, J. Comp. Phys., 65, 292–313 (1986).
18. J.-B. Lagaert, G. Balarac and G.-H. Cottet, *Hybrid spectral particle method for the turbulent transport of a passive scalar*, J. Comp. Phys., 260, 127–142 (2014).
19. M.-S. Liou and C.J. Steffen Jr., *A new flux splitting scheme*, Journal of Computational Physics 107, 23–39 (1993).
20. A. Magni and G.-H. Cottet, *Accurate, non-oscillatory remeshing schemes for particle methods*, J. Comput. Phys., 231 (1), 152–172, (2012).
21. J.E. Martin and E. Meiburg, *Numerical investigation of three-dimensional evolving jets subject to axisymmetric and azimuthal perturbation*, J. Fluid Mech., 230, 271 (1991).
22. J.J. Monaghan, *Particle Methods for Hydrodynamics*, Comp. Phys. Reports, 3, 71–124, (1985).
23. G. Oger, M. Doring, B. Alessandrini, P. Ferrant, *An improved SPH method: Towards higher order convergence*, J. Comp. Phys., 225, 1472–1492 (2007).
24. M.L. Ould-Salihi, G.-H. Cottet, M. El Hamraoui, *Blending finite-differences and vortex methods for incompressible flow computations*, SIAM J. Sci. Comput. 22, 1655–1674 (2000).
25. P. Ploumhans, G.S. Winckelmans, *Vortex methods for high-resolution simulations of viscous flow past bluff bodies of general geometry*, J. Comput. Phys. 165, 354–406 (2000).
26. S. Reboux, B. Schrader and I. Sbalzarini *A self-organizing Lagrangian particle method for adaptive-resolution advectiondiffusion simulations*, J. Comp. Phys, 23, 3623–3646 (2012).
27. G. Russo and J.A. Strain, *Fast triangulated vortex methods for the 2D Euler equations*, J. Comp. Phys., 111, 291–323 (1994).
28. L. Weynans and A. Magni, *Consistency, accuracy and entropic behavior of remeshed particle methods*, ESAIM: Mathematical Modelling and Numerical Analysis, 47, 57–81 (2013).